

Spin Dynamics and Relaxation II: Multilayers and Thin Films

Robert McMichael, Chariman

Semiclassical theory of spin transport in magnetic multilayers

R. Urban,^{a)} B. Heinrich, and G. Woltersdorf

Simon Fraser University, 8888 University Drive, Burnaby, British Columbia V5A 1S6, Canada

(Presented on 15 November 2002)

A semiclassical model of the spin momentum transfer in ferromagnetic film (FM)/normal metal (NM) structures is presented. It is based on the Landau–Lifshitz equation of motion and the exchange interaction in FM, and on the spin diffusion equation in NM. The internal magnetic field is treated by employing Maxwell’s equations. A precessing magnetization in FM creates a spin current which is described by spin pumping proposed by Tserkovnyak *et al.* The back flow of spins from NM into FM is assumed to be proportional to the spin accumulation in NM as proposed by Silsbee *et al.* These theoretical calculations are tested against the experimental results obtained by different groups. A good agreement was found for Py/Cu samples, but spin pumping is significantly enhanced in Py/Pt systems. © 2003 American Institute of Physics. [DOI: 10.1063/1.1555374]

In our recent ferromagnetic resonance (FMR) studies^{1–4} it was shown that the transfer of the spin momentum across ferromagnetic (FM)/normal metal (NM) interfaces can result in nonlocal interface Gilbert damping G' . The generation of spin momentum in magnetic ultrathin films was theoretically described by Tserkovnyak *et al.*⁵ and the effect was called “spin pumping.” The presence of a second magnetic layer creates a spin sink.^{3,4,6,7} The combination of spin pump and spin sink in the ballistic limit leads to an additional interface Gilbert damping. In this article we extend the spin pump and spin sink mechanisms to the nonballistic electron transport which includes a full treatment of the Landau–Lifshitz (LL) equation of motion in FM and diffusion equation in NM and Maxwell’s equations accounting for a finite penetration of the rf fields.

The coordinate system was chosen in such a way that the sample normal is parallel to the z axis. The external dc field, \mathbf{H} , lies in the sample plane and is parallel to the y axis, and the internal electromagnetic rf fields are $\mathbf{h}=(h,0,0)$, $\mathbf{e}=(0,e,0)$. The LL equations of motion in FM and NM layers can be written as

$$\frac{1}{\gamma} \frac{\partial \mathbf{M}^F}{\partial t} = -(\mathbf{M}^F \times \mathbf{H}_{\text{eff}}^F) + \frac{G_0}{\gamma^2 M_s^2} \left(\mathbf{M}^F \times \frac{\partial \mathbf{M}^F}{\partial t} \right), \quad (1)$$

$$\frac{1}{\gamma} \frac{\partial \mathbf{M}^N}{\partial t} = -(\mathbf{M}^N \times \mathbf{H}_{\text{eff}}^N) + \frac{D}{\gamma} \nabla^2 \mathbf{M}^N - \frac{\delta \mathbf{M}^N}{\gamma \tau_{sf}}, \quad (2)$$

where γ is the absolute value of the electron gyromagnetic ratio, M_s is the saturation magnetization of FM, G_0 is the intrinsic Gilbert damping, D is the diffusion constant in NM ($D=v_F^2 \tau_{el}/6$, v_F is the Fermi velocity and τ_{el} is the electron momentum relaxation time), τ_{sf} is the spin–flip relaxation

time, and $\delta \mathbf{M}^N = \mathbf{M}^N - \chi_P \mathbf{h}$ is the excess magnetization in NM, where χ_P is the Pauli susceptibility. The effective field $\mathbf{H}_{\text{eff}}^F$ is derived from the total Gibbs free energy which contains the external fields, magnetocrystalline anisotropies, and exchange interaction.⁸ The effective field $\mathbf{H}_{\text{eff}}^N$ in NM contains only the external dc, internal field \mathbf{H} , and the demagnetizing field perpendicular to the sample plane. Equations (1) and (2) were solved in a small angle approximation using

$$\mathbf{M}^F = (m_x^F, M_s, m_z^F), \quad (3)$$

$$\delta \mathbf{M}^N = (m_x^N - \chi_P h, \chi_P H, m_z^N), \quad (4)$$

where H is the external applied magnetic field. The time and spatial variations of the rf components were assumed to be $\sim \exp(i\omega t - kz)$, where k is the propagation wave vector and ω is the rf angular frequency. Maxwell’s equations in Gaussian units neglecting the displacement current for this geometry are

$$-4\pi k_0^2 i m_x + (k^2 - i k_0^2) h = 0, \quad (5)$$

$$\frac{e}{h} = k \frac{c}{4\pi\sigma}, \quad b_z = 0, \quad (6)$$

where σ is the appropriate conductivity, c is the velocity of light in free space, and $k_0^2 = (4\pi i \sigma \omega)/c^2$. The skin depth $\delta = c/\sqrt{(2\pi\sigma\omega)}$.

Equations (1), (2), (5), and (6) provide the secular equation for k . In both cases, FM and NM, the secular equation results in a cubic equation in k^2 which leads to six k wave numbers with corresponding six waves of propagation. The rf magnetization and electromagnetic field components are given by a linear superposition of six waves. The coefficients are evaluated by matching the boundary conditions at the film interfaces.

^{a)}Electronic mail: rurban@sfu.ca

We assume no direct exchange interaction between the FM and NM layers. The coupling between FM and NM is caused by spin currents across the FM/NM interface. We consider three contributions to the net spin flow:

$$\mathbf{I}_{\text{FM} \rightarrow \text{NM}} = \frac{\hbar g^{\uparrow\downarrow}}{4\pi M_s^2} \left(\mathbf{M}^F \times \frac{\partial \mathbf{M}^F}{\partial t} \right), \quad (7)$$

$$\mathbf{I}_{\text{NM} \rightarrow \text{FM}} = \frac{v_F t_{\text{NM}}}{4\gamma} \delta \mathbf{M}^N, \quad (8)$$

$$\mathbf{I}_{\text{diff}} = \frac{Dk}{\gamma} \delta \mathbf{M}^N. \quad (9)$$

$\mathbf{I}_{\text{FM} \rightarrow \text{NM}}$ is described by the spin pumping model proposed by Tserkovnyak *et al.*^{5,9} Parameter $g^{\uparrow\downarrow}$ represents is the number of conducting channels per unit area⁹ which is directly related the interface mixing conductance $G^{\uparrow\downarrow}$ by

$$g^{\uparrow\downarrow} = \frac{h}{e^2} G^{\uparrow\downarrow}, \quad (10)$$

where e is the electron charge, and h is Planck's constant. $G^{\uparrow\downarrow}$ were evaluated for different interfaces by first principle band calculations by Xia *et al.*¹⁰

$\mathbf{I}_{\text{NM} \rightarrow \text{FM}}$ was proposed by Silsbee *et al.*^{11,12} from a simple kinematic argument. t_{NM} is the transmission coefficient for conduction electrons from NM into FM. Tserkovnyak *et al.* used for $\mathbf{I}_{\text{NM} \rightarrow \text{FM}}$ a similar term (I_s^{back} in their notation). The transmission coefficient t_{NM} can be determined by direct comparison of $\mathbf{I}_{\text{NM} \rightarrow \text{FM}}$ and I_s^{back} (Ref. 9) and is found to be

$$t_{\text{NM}} = \pi \frac{g^{\uparrow\downarrow}}{k_F^2}, \quad (11)$$

where k_F is the Fermi wave vector. Note, that the coefficient in Eq. (7) and t_{NM} are proportional to the number of conducting channels, which reduces the number of free fitting parameters. Since $g^{\uparrow\downarrow} \approx k_F^2/4\pi$,¹³ the transmission coefficient is ≈ 0.25 .

\mathbf{I}_{diff} is present only in NM. It represents the flux of non-equilibrium spins away from the FM/NM interface into the NM bulk. $\delta \mathbf{M}$ relaxes back to equilibrium with the rate of $1/\tau_{sf}$.

At each interface there are two electromagnetic boundary conditions (continuity of h and e). In addition, the following four boundary conditions satisfy the magnetic and spin flow requirements at the FM/NM and NM/FM interfaces.

FM:

$$\left(-\frac{2A}{M_s} k - \frac{K_s}{M_s} \right) M_z + I_{\text{FM} \rightarrow \text{NM}}^{(x)} = I_{\text{NM} \rightarrow \text{FM}}^{(x)}, \quad (12)$$

$$\frac{2A}{M_s} k M_x + I_{\text{FM} \rightarrow \text{NM}}^{(z)} = I_{\text{NM} \rightarrow \text{FM}}^{(z)},$$

where A is the strength of the bulk exchange coupling and K_s is the interface perpendicular uniaxial anisotropy ($E_s = -K_s \cos^2(\theta)$ [erg/cm²]), see Ref. 8. The term in the round

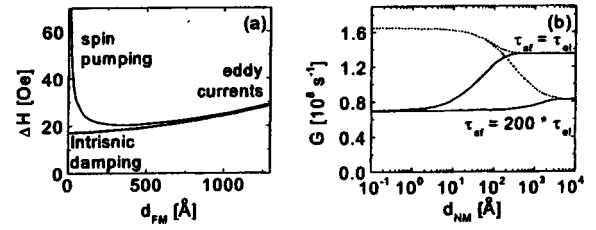


FIG. 1. (a) Total FMR linewidth ΔH as a function of d_{FM} at $f = 10$ GHz. Calculations were carried out for FM using permalloy (Py, Ni₈₀Fe₂₀, $4\pi M_s = 10.7$ kOe, $G_0 = 0.7 \times 10^8$ s⁻¹, $\rho = 15$ μΩ cm) and NM using Cu ($\rho = 1$ μΩ cm, $\tau_{el} = 2.5 \times 10^{-14}$ s, $D = 95$ cm²/s). The dashed line corresponds to a single Py layer and therefore ΔH is caused by the bulk properties. The solid line shows the linewidth which includes spin pumping ($g^{\uparrow\downarrow} = 1 \times 10^{15}$ cm⁻²), assuming a perfect sink at the FM/NM interface ($t_{\text{NM}} = 0$). (b) ΔH as a function of the NM thickness for two different values of τ_{sf} . The solid lines correspond to a perfect mirror at the back side of NM [$d(\delta M)/dz = 0$]. The dashed lines correspond to a perfect spin sink at the back side of NM ($\delta M = 0$).

bracket arises from the interface torques generated by the exchange coupling and the interface perpendicular uniaxial anisotropy.

NM:

$$\mathbf{I}_{\text{FM} \rightarrow \text{NM}} = \mathbf{I}_{\text{NM} \rightarrow \text{FM}} + \mathbf{I}_{\text{diff}}. \quad (13)$$

The calculations were carried out for symmetric driving. This means that the rf components of \mathbf{h} at both outer surfaces are equal.

It is interesting to explore the following aspects of the above theory:

(A) The strength of $g^{\uparrow\downarrow}$: $g^{\uparrow\downarrow}$ can be found in Ref. 10 and ranges between 1 and 2×10^{15} cm⁻². In the limit of $t_{\text{NM}} \rightarrow 0$ there is no backflow of the spin momentum from NM into FM. This corresponds to a “perfect spin sink” and gives the maximum effect regardless of d_{NM} (thickness of NM), D , and τ_{sf} .

(B) FMR linewidth, ΔH vs d_{FM} : Figure 1(a) shows the total FMR linewidth as a function of the FM layer thickness d_{FM} . The dotted line does not include spin pumping ($g^{\uparrow\downarrow} = 0$). In this case, there are two regions: (i) For $d_{\text{FM}} < 300$ Å ΔH is dominated by the intrinsic damping G_0 of a single layer; (ii) for $d_{\text{FM}} > 500$ Å the additional broadening arises from eddy currents. The solid line includes spin pumping ($g^{\uparrow\downarrow} = 1 \times 10^{15}$ cm⁻²). Amazingly, the additional broadening *always* scales like $1/d_{\text{FM}}$. For $d_{\text{FM}} > 500$ Å the additional interface damping is negligible (ΔH with and without $g^{\uparrow\downarrow}$ are within 1 Oe).

(C) G vs d_{NM} , influence of λ_{sf} : In Fig. 1(b) the solid lines represent calculated total Gilbert damping G assuming a perfect mirror at the back side of NM [$d(\delta M)/dz = 0$]. For $d_{\text{NM}} \ll \lambda_{sf} = v_F \sqrt{\tau_{el} \tau_{sf}} / 6$ the rf magnetization accumulates in NM and the spin current $\mathbf{I}_{\text{NM} \rightarrow \text{FM}}$ compensates the spin pumping current $\mathbf{I}_{\text{FM} \rightarrow \text{NM}}$ resulting in zero interface damping ($G = G_0$). When d_{NM} becomes comparable to λ_{sf} the spin current $\mathbf{I}_{\text{NM} \rightarrow \text{FM}}$ is not sufficient to compensate $\mathbf{I}_{\text{FM} \rightarrow \text{NM}}$ resulting in increased Gilbert damping. This increase eventually saturates and its final value depends on the ratio of τ_{el} / τ_{sf} . The dashed line in Fig. 1(b) represents a perfect spin sink at the back side of NM ($\delta M = 0$). Note, that in this case

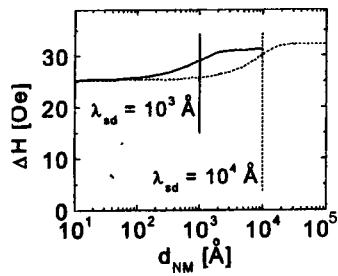


FIG. 2. ΔH for Py (20 Å) covered by Cu(d_{NM}) for RT (solid line) and a cryogenic temperature (dashed line) with the resistivity ratio equal to 10. Calculations were carried out at $f=10$ GHz. For RT $\tau_{\text{el}}=2.5 \times 10^{-14}$ s and $\epsilon=\tau_{\text{sf}}/\tau_{\text{el}}=100$. ϵ was assumed to be temperature independent.

for $d_{\text{NM}} \ll \lambda_{\text{sf}}$ one obtains a perfect spin sink (equivalent to $t_{\text{NM}}=0$) and for a large Cu thickness there is no difference between the Cu/ perfect-sink and Cu/ perfect-mirror.

(D) Influence of the skin depth δ : It is interesting to discuss the limit when the skin depth δ becomes comparable or even less than λ_{sf} . Figure 2 simulates the effect of decreasing temperature. The solid line corresponds to Py/Cu at room temperature (RT), and the dashed line corresponds to a cryogenic temperature (CT) with the resistivity ratio equal to 10. In this calculation the ratio between τ_{el} and τ_{sf} was assumed to be temperature independent. The spin diffusion lengths for RT and CT are 0.1 and 1 μm , respectively. The corresponding skin depths are 0.5 and 0.2 μm , respectively. For RT the ratio $R=\delta/\lambda_{\text{sf}} \approx 5$ while for CT $R \approx 1/6$. Note, that in both cases the additional linewidth increases when d_{NM} becomes comparable to λ_{sf} , and saturates for $d_{\text{NM}} \ll \lambda_{\text{sf}}$.

In the remainder of this article some recent experimental results will be discussed. Mizukami *et al.*¹⁴ and Invarsson *et al.*¹⁵ investigated the FMR linewidth in Py films which were surrounded by NM layers. In both cases they observed an interface damping. Their studies were carried out at different microwave frequencies. The strength of the interface damping in the same type of samples (Pt/Py/Pt) scaled with the microwave frequency. It is, therefore, appropriate to interpret their results using the spin pumping theory as outlined above. The strength of the interface damping in the Py films surrounded by Pt and Pd is surprisingly high. Even for the case when these layers act as perfect sinks ($t_{\text{NM}}=0$) one needs to use $g^{\uparrow\downarrow}=2.5$ and $1.4 \times 10^{15} \text{ cm}^{-2}$ for Pt and Pd, respectively. The number of transversal channels for light electrons ($m^*/m_{\text{el}} \approx 2$) of the sixth band¹⁶ is the same for Pt and Pd and leads to $g^{\uparrow\downarrow}=0.7 \times 10^{15} \text{ cm}^{-2}$. This number can be perhaps enhanced by a factor of 2 by including the heavy holes. Therefore, one can expect $g^{\uparrow\downarrow}$ to be in a range between 0.7 to $1.4 \times 10^{15} \text{ cm}^{-2}$. This is clearly at variance with the experimental value for Pt ($2.5 \times 10^{15} \text{ cm}^{-2}$). A possible explanation is being offered by the Stoner enhancement factor which enhances the strength of spin pumping, see Simanek and Heinrich.¹⁷

Recently we studied the increase of the Gilbert damping in GaAs/16Fe/10Pd/20Au(001), where integers represent the number of atomic layers. This sample was prepared by molecular beam epitaxy (MBE) where atomic intermixing be-

tween Fe and Pd is kept at its minimum. The additional Gilbert damping at $f=24$ GHz was found to be $0.3 \times 10^8 \text{ s}^{-1}$. This value is small compared to the increase in G ($1.7 \times 10^8 \text{ s}^{-1}$) that was measured by Mizukami *et al.*¹⁴ for the same FM thickness. In interpretation of our data we have to invoke a finite spin diffusion length. The required value is $\lambda_{\text{sf}}=70$ Å. However, that needs $\tau_{\text{sf}}=\tau_{\text{el}}$ which we find unrealistic. The mean free path exceeds significantly the Pd thickness; therefore, we are in the ballistic limit where our theory does not apply. In the ballistic limit it is more reasonable to interpret the measured data by determining the fraction of $I_{\text{FM} \rightarrow \text{NM}}$ which was absorbed in Pd. In Mizukami's experiment everything is absorbed, in our measurements only 20% is lost in Pd.

In separate experiments Mizukami *et al.*¹⁸ studied the Gilbert damping as a function of d_{Cu} (from 10 nm to over 1 μm) in glass/Cu(5 nm)/Py/Cu(d_{Cu}) and glass/Cu(5 nm)/Py(3 nm)/Cu(d_{Cu})/Pt samples. Their results are similar to those shown in Fig. 1(b) for $\tau_{\text{sf}}=200 \tau_{\text{el}}$ ($\lambda_{\text{sf}}=0.2 \mu\text{m}$). Notice, that Cu on its own is a poor spin sink even for $d_{\text{Cu}} \gg \lambda_{\text{sf}}$. In glass/Cu/Py/Cu(d_{Cu})/Pt structures one was able to explore the role of the Pt layer when separated from Py by a variable thickness of Cu. The experimental results were possible to explain by assuming that the Cu/Pt interface acted as a perfect spin sink and therefore the increase in the Gilbert damping can be explained by the maximum strength of spin pumping in Cu.

The authors thank Y. Tserkovnyak, E. Simanek, and J. F. Cochran for valuable discussions. Financial support from the Natural Sciences and Engineering Research Council of Canada (NSERC) and Canadian Institute for Advanced Research (CIAR) is gratefully acknowledged. G.W. thanks the German Academic Exchange Service (DAAD) for a generous scholarship.

¹R. Urban, G. Woltersdorf, and B. Heinrich, Phys. Rev. Lett. **87**, 217204 (2001).

²B. Heinrich, R. Urban, and G. Woltersdorf, J. Appl. Phys. **91**, 7523(2002).

³B. Heinrich, R. Urban, and G. Woltersdorf, IEEE Trans. Magn. **38**, 2496 (2002).

⁴B. Heinrich, G. Woltersdorf, R. Urban, and E. Simanek, J. Appl. Phys. (to be published).

⁵Y. Tserkovnyak, A. Brataas, and G. Bauer, Phys. Rev. Lett. **88**, 117601 (2002).

⁶M. Stiles and A. Zangwill Phys. Rev. B **66**, 014407 (2002).

⁷B. Heinrich, G. Woltersdorf, R. Urban and E. Simanek, J. Magn. Magn. Mater. (in press).

⁸B. Heinrich and J. F. Cochran, Adv. Phys. **42**, 523 (1993)

⁹Y. Tserkovnyak, A. Brataas, and G. Bauer, e-print cond-mat/0208091.

¹⁰K. Xia, J. Kelly, G. B. A. Brataas, and I. Turek, Phys. Rev. B **65**, R220401 (2002).

¹¹R. Silsbee, A. Janossy, and P. Monod, Phys. Rev. B **19**, 4382 (1979).

¹²P. Sparks and R. Silsbee, Phys. Rev. B **35**, 5198 (1987).

¹³A. Brataas, Y. Tserkovnyak, G. Bauer, and B. Halperin e-print cond-mat/0205028.

¹⁴S. Mizukami, Y. Ando, and T. Miyazaki, Jpn. J. Appl. Phys., Part 1 **40**, 580 (2001).

¹⁵S. Invarsson, L. Ritchie, X. Liu, G. Xiao, J. Slonczewski, P. Trouilloud, and R. Koch, e-print cond-mat/02008207.

¹⁶C. Lehmann, S. Sinning, P. Zahn, H. Wonn, and I. Mertig, Fermi surface database (1996-1998), URL <http://www.physik.tu-dresden.de/~fermisur/>.

¹⁷E. Simanek and B. Heinrich, e-print cond-mat/0207471.

¹⁸S. Mizukami, Y. Ando, and T. Miyazaki, J. Magn. Magn. Mater. **239**, 42 (2002).